Covalency effect on cation 2p x-ray absorption spectroscopy in 3d transition-metal oxides

1996 J. Phys.: Condens. Matter 8 5253

(http://iopscience.iop.org/0953-8984/8/28/009)

J. Phys.: Condens. Matter **8** (1996) 5253–5268. Printed in the UK

Covalency effect on cation 2p x-ray absorption spectroscopy in 3d transition-metal oxides

J P Crocombette and F Jollet

CEA, DSM, DRECAM, SRSIM, Centre d'Etudes de Saclay, Bâtiment 462, 91191 Gif-sur-Yvette Cédex, France

Received 27 November 1995, in final form 7 March 1996

Abstract. The influence of covalency on the $L_{2,3}$ spectral shape is studied for 3d transition-metal oxides. We present systematic calculations for cations with d^0 to d^8 configurations. Charge transfer leads to a more complex spectral shape and a change in balance between the main peaks. We also exhibit charge-transfer-induced high-spin-to-low-spin transition. We discuss some phenomenological models that have been suggested to account for covalency effects in the framework of ionic calculations, namely the increase in the crystal field possibly associated with a reduction in intracationic Slater integrals.

1. Introduction

The 3d transition-metal oxides (TMOs) have attracted considerable interest because of the breakdown of the one-electron picture in describing their electronic properties. Owing to progress in experimental techniques, x-ray absorption spectroscopy (XAS) is now regarded as a powerful tool for investigating their electronic structure [1]. Among the TMO x-ray absorption spectra, some are known to be well accounted for by band-structure or multiple-scattering calculations. They correspond to cases where the strong interaction between d electrons does not play an important part, a typical example being the oxygen K edge. On the contrary, cation 2p XAS clearly evidences strong d-electron interactions. In fact, the spectral shape depends mainly on the interplay between the d-orbital crystal field, the d–d and 2p–d electronic interactions and the spin–orbit coupling of the 2p level. These spectra are dominated by nearly atomic phenomena and are routinely accounted for by calculations made in the ionic limit [2, 3]. Although covalency can be quite important in TMOs, little is known about its influence on the $L_{2,3}$ edges. Even if there are some models dealing with charge transfer for cation $L_{2,3}$ edges [4–6], no systematic study of the influence of covalency on cation 2p XAS has been published yet.

We want to tackle this point with the configuration interaction (CI) model that we already used in the study of 2p x-ray absorption spectra for some 3d and 4d TMOs [6–8]. This model takes into account electronic interactions, spin–orbit coupling, crystal field and charge transfer through hopping terms. In this paper we present a study of the effect of charge transfer on 2p XAS of 3d TMO cations with d^0 to d^8 configurations. We first introduce our method and then present our results. The effect of covalency on the spectral shape is described. In view of the spectra, we discuss some phenomenological models that have been suggested to account for the covalency effect in the framework of ionic calculations, namely the increase in the crystal field possibly associated with a reduction in intracationic Slater integrals.

0953-8984/96/285253+16$19.50

2. Presentation of the calculations

Our calculations are based on a semi-empirical cluster approach already presented in [6, 7]. We recall briefly the characteristics of our method. We consider a cluster made of a transition-metal cation surrounded by its oxygen first neighbours. In this work we deal with the specific case of O_h symmetry for the cation. So the cluster contains six oxygen ions in perfect octahedral positions around the central cation. The 2p orbitals of the oxygen atoms and the d and 2p orbitals of the cation are considered. The Hamiltonian of the system takes into account the ionic crystal-field splitting, the intracationic electronic repulsions (i.e. d-electron interactions and electron–core hole interactions) and spin–orbit coupling of 2p and d orbitals of the cation. Charge transfer, between oxygen and cation orbitals as between different oxygen atoms, is calculated through hopping terms. This last term can be switched off in which case the ionic limit is considered. Configurations with more than one ligand hole in the oxygen 2p orbitals have been neglected in the calculations. The Hamiltonian is written in a multielectronic basis made of Slater determinants.

The 2p x-ray absorption spectrum is dominated by dipole-allowed transitions to d and s final states. Because of large wavefunction overlap the d channel is much stronger than the s channel [9]. Subsequently the latter is neglected.

In order to study the influence of covalency on $L_{2,3}$ edges, we considered all the cases of formally d^n cations, from $n = 0$ to $n = 8$ (table 1). Only one type of cation was considered for each d^n case, as it is known that the differences between the parameters of the different d^n cations produce only small differences in x-ray absorption spectra [2, 3]. The d^9 case is not considered in this paper as the 2p x-ray absorption spectrum is in this case very simple. It consists of only two peaks: one for each core-hole state ($2p_{1/2}$ and $2p_{3/2}$).

Table 1. For each d^n configuration (first column) are indicated the following: the cation used in the calculations (second column), the electronic interaction Slater integrals (third to seventh columns) and the d and 2p spin–orbit coupling constants (eighth and ninth columns).

Configuration	Cation	F^2_{dd} (eV)	F^4_{dd} (eV)	F^2_{pd} (eV)	G^1_{pd} (eV)	G^3_{pd} (eV)	ζ_d (eV)	ζ_p (eV)
d^0	Ti^{4+}	10.343	6.499	6.30	4.62	2.63	0.032	3.78
d^1	Ti^{3+}	10.343	6.499	5.581	3.991	2.268	0.027	3.776
d^2	V^{3+}	10.127	6.354	6.057	4.392	2.496	0.036	4.649
d^3	Cr^{3+}	10.777	6.755	5.526	4.788	2.722	0.047	5.667
d^4	Cr^{2+}	9.649	6.002	5.841	4.024	2.388	0.041	5.668
d^5	Mn^{2+}	10.316	6.414	6.321	4.606	2.618	0.053	6.846
d^6	Fe^{2+}	10.966	6.414	6.793	5.004	2.844	0.067	8.200
d^7	Co^{2+}	11.605	7.209	7.260	5.397	3.069	0.083	9.746
d^8	Ni^{2+}	12.234	7.598	7.721	5.787	3.291	0.102	11.507

The ionic crystal-field splitting $10Dq$ was taken to be equal to 1.5 eV. Hopping terms are calculated from the Slater–Koster [10] formulae which involve the common parameters η_σ and η_π [1]. We chose the usual ratio $\eta_\pi = -\frac{1}{2}\eta_\sigma$ and the value of η_σ was fixed to 1.4 eV. For each d^n configuration, the Slater integrals F^2_{dd}, F^4_{dd}, F^2_{pd}, G^1_{pd} and G^3_{pd} appearing in intracationic elements of the Hamiltonian were taken from Hartree–Fock *ab-initio* calculations (table 1) [2, 11], but these values obtained by the one-electron method should be reduced to account for intra-atomic correlations effects before use in CI calculations [12]. We chose a multiplicative factor of 80%. The spin–orbit coupling parameters are taken from the same Hartree–Fock calculations [2, 11] (see table 1).

The $L_{2,3}$ edges of 3d transition-metal compounds may vary with temperature [13]. As the experiments are usually performed at room temperature, a temperature of 300 K is assumed in the calculation. In this case, the distribution weights of the eigenvectors of the Hamiltonian in the equilibrium state follow a Maxwell–Boltzmann law. The ground state of the cluster is written

$$|\varphi_g\rangle = \sum_i a_i |(\mathrm{d}^n)_i\rangle + \sum_j b_j |(\mathrm{d}^{n+1}\underline{\mathrm{L}})_j\rangle.$$

In this expression, i runs over the Slater determinants of the ionic configuration d^n and j runs over the Slater determinants over the one-ligand-hole configuration $\mathrm{d}^{n+1}\underline{\mathrm{L}}$.

The amount of charge transfer, from oxygen orbitals to cation orbitals, in the ground state, is measured by the total weight of the $\mathrm{d}^{n+1}\underline{\mathrm{L}}$ configuration in the ground state.

It is equal to

$$\sum_j |b_j|^2 \Big/ \left(\sum_i |a_i|^2 + \sum_j |b_j|^2 \right).$$

This amount of charge transfer is almost the same for the first excited states of the cluster that appear in the equilibrium state. Indeed, these states differ from the ground state, only in the intracationic (low-energy) arrangements of the d electrons. In the same way the final states are mixtures of Slater determinants of $\underline{\mathrm{c}}\mathrm{d}^{n+1}$ and $\underline{c}\mathrm{d}^{n+2}\underline{\mathrm{L}}$ configurations ($\underline{\mathrm{c}}$ denotes a hole in the cation 2p shell).

Owing to the semi-empirical character of our method, we are able to monitor the charge transfer. The parameter that we use to vary it is the difference between the atomic energies of the cation d and oxygen p orbitals: $\varepsilon_d - \varepsilon_p$. This parameter contributes to the value of the charge transfer energy Δ, defined as the difference between the energies of the lowest states of the d^n and the $\mathrm{d}^{n+1}\underline{\mathrm{L}}$ configurations:

$$\Delta = E^0(\mathrm{d}^{n+1}\underline{\mathrm{L}}) - E^0(\mathrm{d}^n).$$

The value of the E^0 energies depends on $\varepsilon_d - \varepsilon_p$, but also on intracationic electronic interactions (through the Slater integrals), the spin–orbit coupling and the crystal field. The values of $E^0(\mathrm{d}^n)$ are tabulated in [14]. When $\varepsilon_d - \varepsilon_p$ is decreased, Δ is reduced and charge transfer is enhanced. The ionic limit, for which charge transfer is switched off, would correspond to very large values of Δ or $\varepsilon_d - \varepsilon_p$.

For all n from 0 to 8, three cases were considered. Firstly the ionic limit of the pure d^n configuration in the ground state is dealt with. Secondly $\varepsilon_d - \varepsilon_p$ was fixed so that the amount of charge transfer in the ground state is 20%. In the last case the charge transfer is monitored to 40%. The corresponding values of Δ are indicated in table 2. We shall arbitrarily talk about partly and highly covalent for these last two cases. Apart from the value of $\varepsilon_d - \varepsilon_p$, all the other parameters were equal for the three calculations. Typical values of 6 eV and 8 eV have been taken for F^0_{dd} and F^0_{pd}, respectively. So, the effective value of Δ in the final state, $\Delta_f \approx \Delta + F^0_{dd} - F^0_{pd}$, is about 2 eV smaller than the initial-state value.

Covalency can be described from a CI or a one-electron picture. The two points of view are sketched in figures 1 and 2. In the CI picture, covalency creates a mixing between d^n and $\mathrm{d}^{n+1}\underline{\mathrm{L}}$ configuration states, leading to bonding (low-energy) and antibonding (high-energy) states (figure 1). The ground state is then the lowest-energy bonding state. In the same way, final states are mixtures of $\underline{\mathrm{c}}\mathrm{d}^{n+1}$ and $\underline{\mathrm{c}}\mathrm{d}^{n+2}\underline{\mathrm{L}}$ states, resulting in bonding and antibonding states. In the one-electron picture the atomic d orbitals divided into t_{2g} and e_g sets mix with oxygen states to form molecular orbitals which can still be divided into t_{2g}

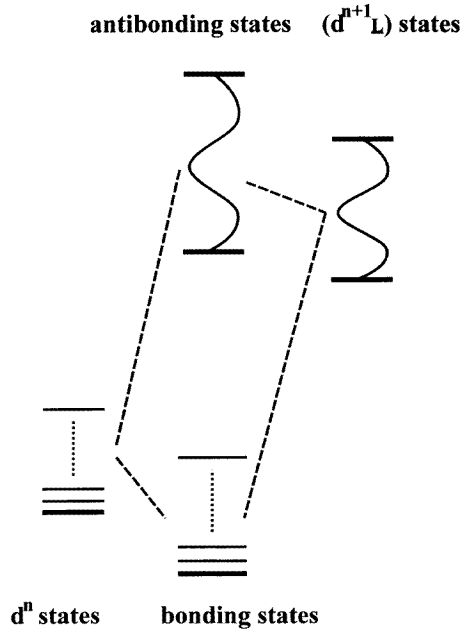

Figure 1. CI point of view for covalency effects. The admixture of d^n and $d^{n+1}\underline{L}$ states creates bonding and antibonding states.

Table 2. For each configuration, d^0 to d^8 values of $\Delta = E^0(d^{n+1}\underline{L}) - E^0(d^n)$ corresponding to an amount of charge transfer of 20% (first column) and 40% (second column) in the ground state.

Configuration	d^0	d^1	d^2	d^3	d^4	d^5	d^6	d^7	d^8
Δ (20%) (eV)	9.6	8.8	8.1	9.4	8.3	8.3	10.8	8.0	9.1
Δ (40%) (eV)	3.3	3.0	3.1	4.9	3.8	3.8	5.7	5.7	5.1

and e_g orbitals. The splitting between the molecular t_{2g} and e_g orbitals is larger than the atomic d orbital splitting induced by the ionic crystal-field only (figure 2).

In figures 3–11 are drawn, for d^0 to d^8, the calculated $L_{2,3}$ spectra of the ionic and the two covalent cases. To account for intrinsic and experimental broadening, a Lorentzian function and a Gaussian function have been convoluted with the calculated poles indicated in the figures. Typical values of 0.4 eV and 0.2 eV have been used for Lorentzian and Gaussian broadenings, respectively. For each configuration, the energy position of the $L_{2,3}$ edge in the x-ray absorption spectrum depends on the depth of the 2p level of the cation. As this energy is not considered in our calculation, the absolute value of the energies on the *X* axis is arbitrary. In order to allow comparison between the different covalencies the curves have then been shifted so that their main peaks are aligned. Moreover, it is known [15] that the area of an $L_{2,3}$ edge is proportional to the number of holes in the d shell prior to the absorption process. To ease the comparison between the spectra of the different (d^n) configurations, all the spectra have been renormalized to have equal areas.

To describe the general features of the effect of charge transfer on the spectra, one can firstly say that, compared with the ionic spectra, the balance between the main peaks appears to be modified by charge transfer.

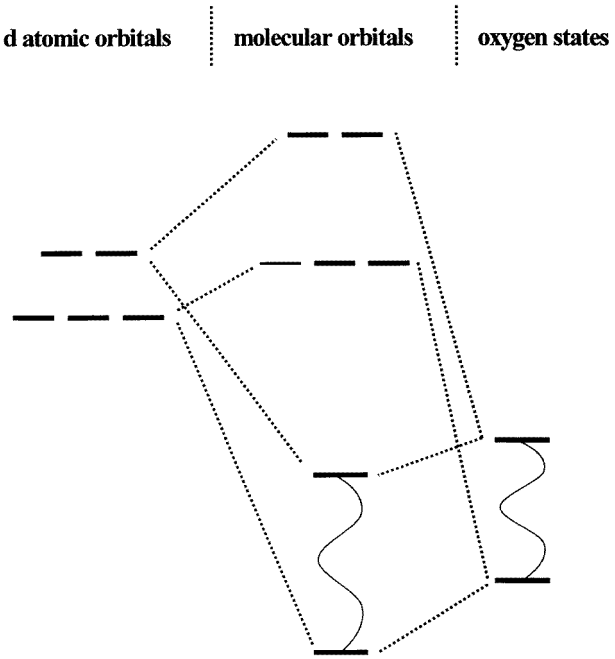

Figure 2. Single-electron point of view for covalency effects. The atomic d orbitals hybridize with oxygen state orbitals, leading to molecular orbitals, for which the t_{2g}–e_g splitting is larger than for the atomic orbitals.

Supplementary poles also appear on the high-energy side of the spectra. Although high-energy structures are already visible in the ionic calculations, some more are present in the covalent spectra. Generally speaking the covalent spectra present more peaks and are more complex than the ionic spectra. These trends are more visible on the L_2 edge, i.e. on the higher-energy side (right-hand part), than on the L_3 edge (left-hand part), on the lower-energy side of the spectra.

d^6 and d^7 spectra exhibit strong differences between ionic and covalent spectra due to high-spin-to-low-spin transition in the ground state. We postpone the study of these two cases on which we shall focus in section 4. The d^8 case also deserves particular attention (see section 5).

We first consider the d^0 to d^5 spectra. The general arguments developed in this part can also be applied to the other cases.

3. The d^0 to d^5 cases and the enhancement of the crystal field

The d^0 to d^5 spectra exhibit soft continuous changes when covalency is increased. To account for the increased complexity of the spectra, one should consider, from the CI point of view, the supplementary peaks that appear when covalency is taken into account; the admixture, in the final state, between cd^{n+1} and $cd^{n+2}\underline{L}$ configuration states creates bonding (low-energy) and antibonding (high-energy) states (see figure 1). Compared with an ionic calculation where only the bonding states exist, the antibonding final states create, in the covalent calculation, supplementary peaks which form charge-transfer satellites. Unlike core-level XPS, charge-transfer satellites are small in x-ray absorption spectra because the

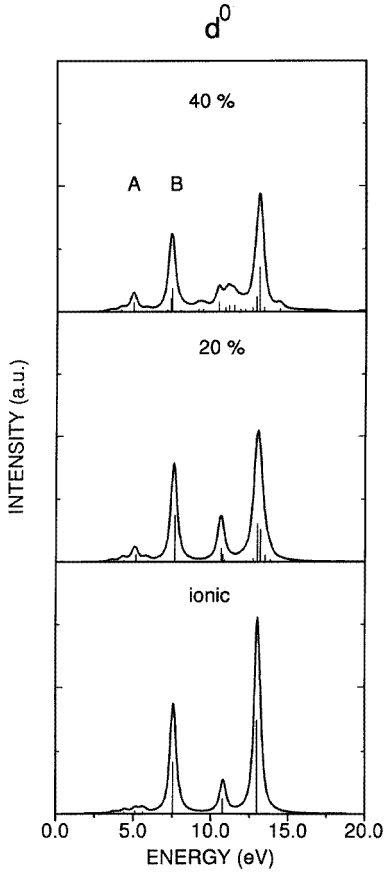

Figure 3. Calculated poles and broadened spectra for d^0 $L_{2,3}$ edges (a.u., arbitrary units): lower curve, ionic spectrum; middle curve, partly covalent spectrum (20% weight of $d^{n+1}\underline{L}$ configurations); upper curve, highly covalent spectrum (40% weight of $d^{n+1}\underline{L}$ configurations).

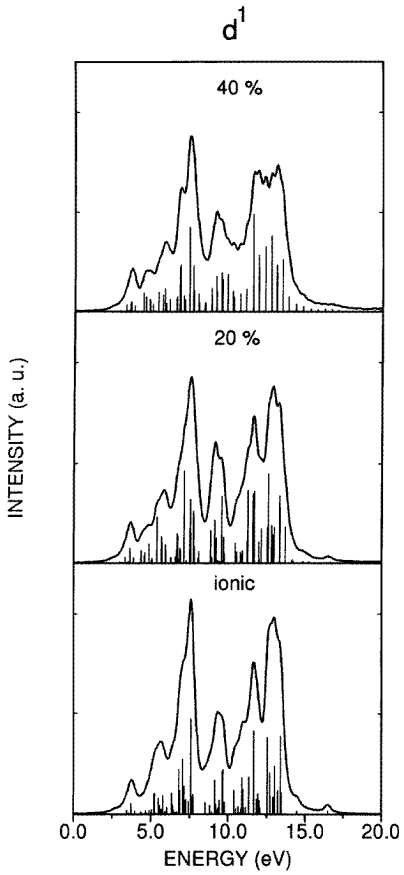

Figure 4. Calculated poles and broadened spectra for d^1 $L_{2,3}$ edges (a.u., arbitrary units): lower curve, ionic spectrum; middle curve, partly covalent spectrum (20% weight of $d^{n+1}\underline{L}$ configurations); upper curve, highly covalent spectrum (40% weight of $d^{n+1}\underline{L}$ configurations).

change in covalency between the initial and final states is small. Indeed Δ_f is quite close to Δ. These small charge-transfer satellites can be seen in the high-energy part of the spectra where supplementary poles appear with increasing covalency and form tails in the spectra. For these high energies, they are not hidden by other peaks. Similar poles and tails exist in lower-energy parts of the spectra, but they cannot be seen independently from the predominant bonding-states peaks that appear at the same energy. For these energies they are responsible for the complex nature of the spectral shape. Such supplementary peaks can by no means be obtained by ionic calculations which indicates that d^n covalent spectra cannot be represented as a superposition of the d^n and d^{n+1} ionic spectra.

Charge transfer creates antibonding peaks, but it also changes the structure of bonding states compared with ionic states. Both initial and final bonding states are modified by charge transfer. This explains the large change in balance between the main peaks in ionic and covalent spectra. For instance, such an effect is clearly visible in the increase in the first

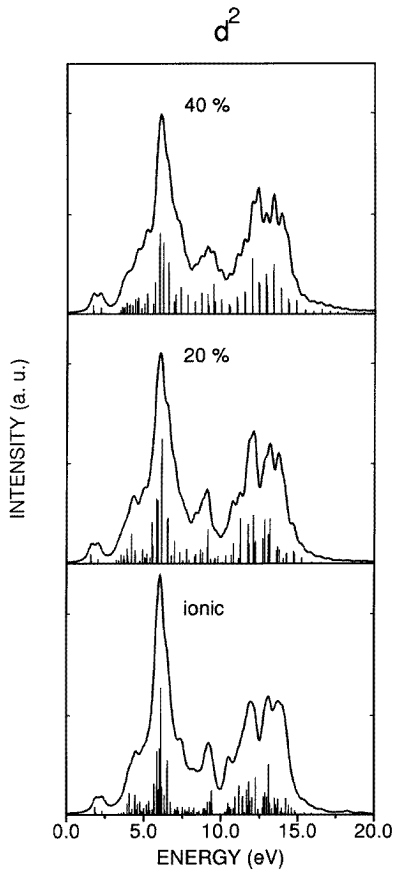

Figure 5. Calculated poles and broadened spectra for d^2 $L_{2,3}$ edges (a.u., arbitrary units): lower curve, ionic spectrum; middle curve, partly covalent spectrum (20% weight of $d^{n+1}\underline{L}$ configurations); upper curve, highly covalent spectrum (40% weight of $d^{n+1}\underline{L}$ configurations).

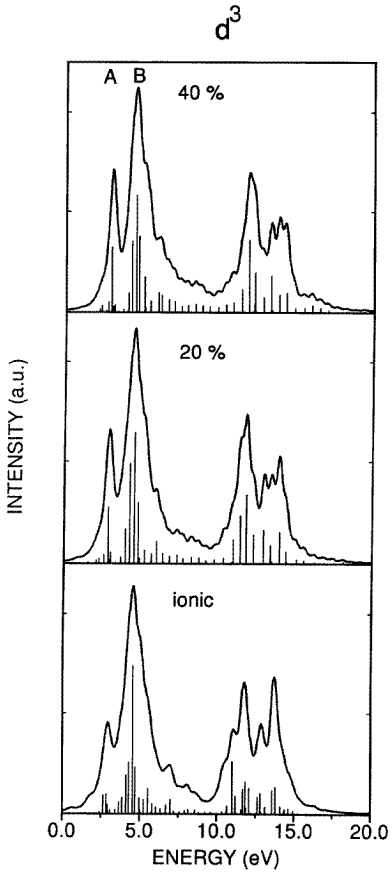

Figure 6. Calculated poles and broadened spectra for d^3 $L_{2,3}$ edges (a.u., arbitrary units): lower curve, ionic spectrum; middle curve, partly covalent spectrum (20% weight of $d^{n+1}\underline{L}$ configurations); upper curve, highly covalent spectrum (40% weight of $d^{n+1}\underline{L}$ configurations).

peak of the L_3 edge (labelled A in the figures) compared with the close main peak (labelled B in the figures) in d^0, d^3 and d^5 configurations. The associated splitting of these two peaks also exhibits a small increase when the charge transfer increases. In the one-electron picture (figure 2), this increase in the splitting is equivalent to the larger separation of d molecular orbitals compared with atomic orbitals split only by the crystal field. The inclusion of charge transfer also reduces the relative influence of multielectronic interactions compared with the other terms, namely the crystal field and charge transfer. The intensity ratio of peak A to peak B is thus slightly closer to the single-particle limit, without electronic interactions, for which it would correspond to the number of holes in the t_{2g} and e_g orbitals. So the first peak becomes increasingly higher as the covalency increases. A similar effect is observed for these spectra when the crystal field is increased in ionic calculations [2, 3].

An open question is then the possibility of reproducing the covalent spectra with purely ionic calculations by increasing the crystal field.

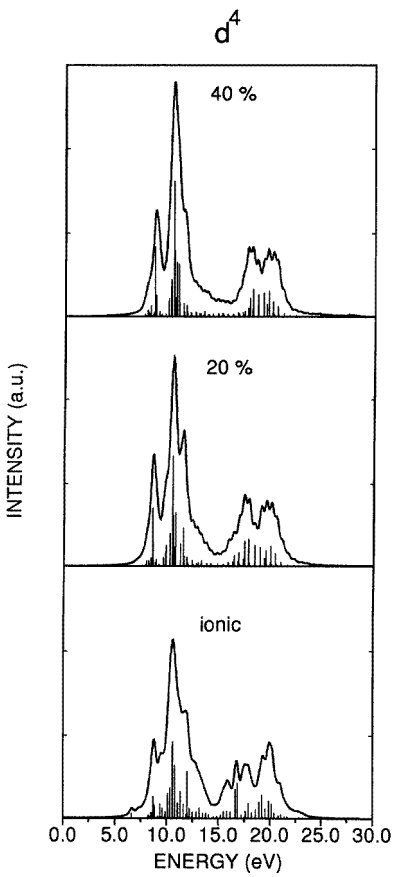

Figure 7. Calculated poles and broadened spectra for d^4 $L_{2,3}$ edges (a.u., arbitrary units): lower curve, ionic spectrum; middle curve, partly covalent spectrum (20% weight of $d^{n+1}\underline{L}$ configurations); upper curve, highly covalent spectrum (40% weight of $d^{n+1}\underline{L}$ configurations).

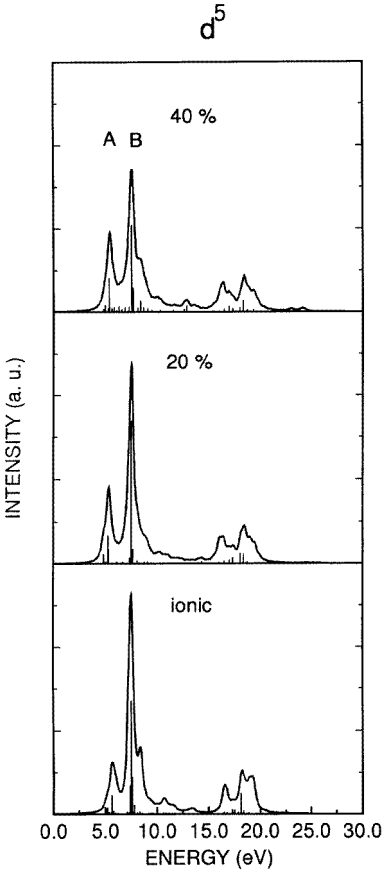

Figure 8. Calculated poles and broadened spectra for d^5 $L_{2,3}$ edges (a.u., arbitrary units): lower curve, ionic spectrum; middle curve, partly covalent spectrum (20% weight of $d^{n+1}\underline{L}$ configurations); upper curve, highly covalent spectrum (40% weight of $d^{n+1}\underline{L}$ configurations).

To check this point we made a series of ionic calculations, slowly increasing the crystal field from the lower value of 1.5 eV used in the preceding calculations up to 3 eV. We do not show the spectra obtained as the reader can refer to [2, 3] for a systematic study of the effect of crystal field on spectral shape. The direct comparison between our curves and those of these references should be handled cautiously as we did not choose the same broadenings as theirs.

Having calculated all these ionic spectra, we compared them with the covalent calculations for each d^n cation. Of course no ionic spectra would exactly fit the covalent calculations, as they do not exhibit charge-transfer satellites. Nevertheless, spectra close to the partly covalent 20% $d^{n+1}\underline{L}$ calculation can be found for the d^0 to d^5 configurations. The corresponding value of crystal-field splitting is approximately 2 eV in all cases considered. This value is to be compared with the crystal field considered in the covalent calculations which was $10Dq = 1.5$ eV.

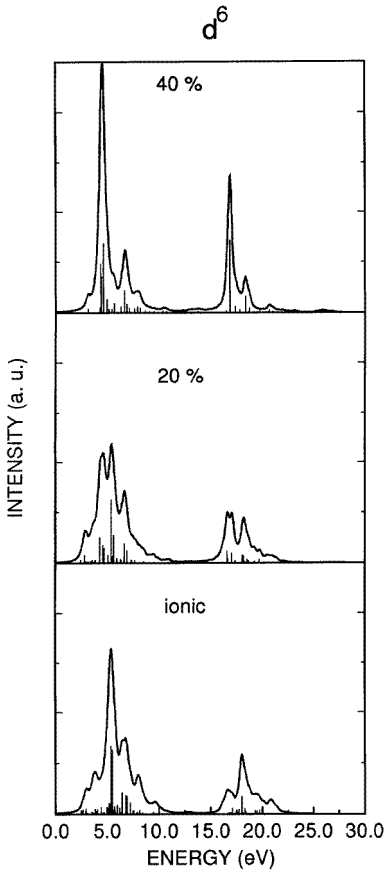

Figure 9. Calculated poles and broadened spectra for d^6 $L_{2,3}$ edges (a.u., arbitrary units): lower curve, ionic spectrum; middle curve, partly covalent spectrum (20% weight of $d^{n+1}\underline{L}$ configurations); upper curve, highly covalent spectrum (40% weight of $d^{n+1}\underline{L}$ configurations).

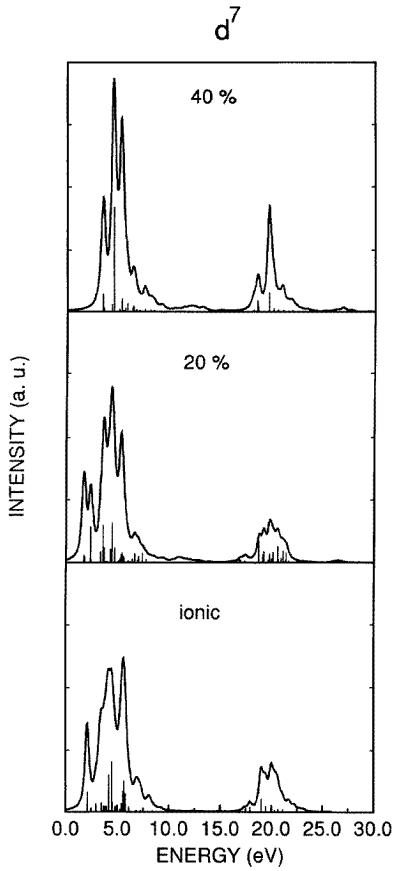

Figure 10. Calculated poles and broadened spectra for d^7 $L_{2,3}$ edges (a.u., arbitrary units): lower curve, ionic spectrum; middle curve, partly covalent spectrum (20% weight of $d^{n+1}\underline{L}$ configurations); upper curve, highly covalent spectrum (40% weight of $d^{n+1}\underline{L}$ configurations).

When the highly covalent 40% $d^{n+1}\underline{L}$ spectra are considered, it proves more difficult to find similar ionic spectra. The complexity of the spectra is so important that it is not possible to establish a correspondence between the highly covalent spectra and any of the ionic spectra. We can conclude that the effect of covalency is only partly reproduced by an increase in the crystal field in the framework of ionic calculations. In fact the trends explained by the relative decrease in electron–hole interactions are roughly reproduced when one increases the crystal field in ionic calculations, but increased complexity of the spectra cannot be achieved by increasing the crystal field.

4. High-spin-to-low-spin transition in the d^6 and d^7 cases

It has already been highlighted that, for the d^6 and d^7 configurations, a high-spin-to-low-spin transition occurs when the charge transfer is increased. We present a detailed study

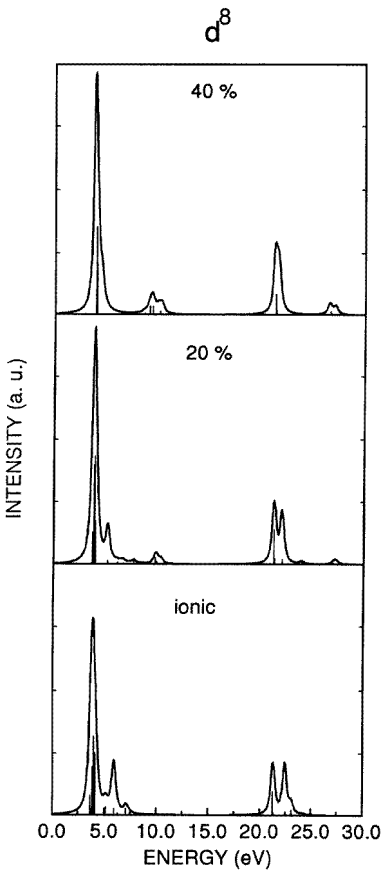

Figure 11. Calculated poles and broadened spectra for d^8 $L_{2,3}$ edges (a.u., arbitrary units): lower curve, ionic spectrum; middle curve, partly covalent spectrum (20% weight of $d^{n+1}\underline{L}$ configurations); upper curve, highly covalent spectrum (40% weight of $d^{n+1}\underline{L}$ configurations).

of these two cases because they show nice examples of ground-state and spectral shape changes induced by charge transfer. The high-spin-to-low-spin transition is a ground-state effect that can be tracked in the spectral shape. Increasing the charge transfer increases the number of electrons on the d orbitals, but this rise is not responsible for the spin transition. The transition is due to the difference between the charge-transfer-induced t_{2g} and e_g molecular orbitals, compared with the atomic d orbitals. In a purely ionic model, such transitions are explained by the change in the ratio of crystal-field splittings and electronic interactions; starting from a high-spin situation an increase in the crystal field induces a transition to a low-spin state (figure 12). In our case, the crystal field is kept constant. So the supplementary division induced by the inclusion of charge transfer is responsible for the transition.

The d^6 and d^7 ionic spectra correspond to a high-spin ground state; the highly covalent spectra (40% $d^{n+1}\underline{L}$, upper curve) correspond to a low-spin ground state. The partly covalent curve (20% $d^{n+1}\underline{L}$, middle curve) corresponds to an intermediate situation where the low- and high-spin states have nearly the same energies in the equilibrium state. In this last case, the S_z expectation value, for the equilibrium state, proves to be intermediate between

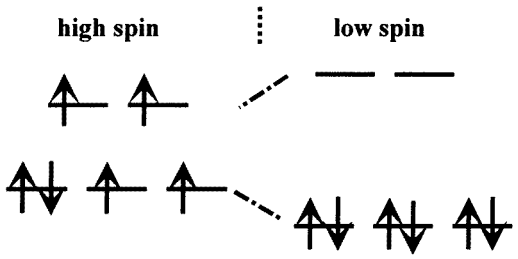

Figure 12. Ionic high-spin-to-low-spin transition in the d^6 case. On the left appears the high-spin ground state. On the right, the splitting of t_{2g} and e_g orbitals is enlarged, which produces a low-spin ground state.

the high-spin and low-spin values (table 3). These two partly covalent states of the d^6 and d^7 cases will hereafter be referred to as the covalent near-transition states. The spin transition produces dramatic changes in the spectra as can be seen in figures 9 and 10. The overall shapes of the high-spin (ionic) and low-spin (highly covalent) spectra are the same as obtained in the framework of ionic calculations when the spin transition is achieved by increasing the crystal field [2, 3].

We compared the covalent high-spin-to-low-spin transition with that created by a rise in crystal field in the framework of ionic calculations. To reproduce an ionic transition, we increased, in the framework of ionic calculations, the crystal-field splitting up to a value δ_i for which the S_z expectation value in the room-temperature equilibrium state has the same value as in the covalent near-transition state. This enables us to define an ionic near-transition state. We then have two different near-transition states to be compared: the covalent state and the ionic state. They have the same S_z-value and so they represent the same stage in the high-spin-to-low-spin transition.

The comparison of the ionic and covalent near-transition states will enable us to deal with the question of the reproducibility of the covalency effect in the framework of ionic calculations by reducing the Slater integrals from their values calculated for isolated ions. Indeed, it is sometimes claimed that a reduction in the Slater integrals and a concomitant increase in the crystal-field splitting can reproduce the effect of covalency in the framework of ionic calculations (this reduction should not be confused with that applied when the Slater integrals are calculated within the Hartree–Fock method (see section 2)). Such a reduction is commonly applied in $L_{2,3}$ edge calculations in order to reproduce an experimental spectrum. For examples of reduction in ionic calculations see [3, 16–18]. It has been shown to have a relation to the nephelauxetic effect in transition-metal complexes, as analysed and shown for instance by Jørgensen [19]. The nephelauxetic effect is defined as the reduction in the Slater integrals of the d orbitals involved in a covalent bonding compared with their ionic values. The reduction accounts for a modification of the shape of the radial distribution of the d orbitals in the complex compared with the isolated ion.

To tackle the applicability of such a reduction in describing covalency effects, we compare the ionic and covalent near-transition states. We have calculated, in both the d^6 and the d^7 covalent near-transition states, δ, which is defined as the total splitting between molecular t_{2g} and e_g orbitals coming from both the crystal field and the charge transfer. δ is the splitting between the molecular orbitals formed by the admixture of atomic cation d and oxygen 2p orbitals. The calculated values of δ for the d^6 and d^7 cases are given in

table 4. As expected, we found δ to be larger than $10Dq = 1.5$ eV which is the ionic crystal-field splitting. In table 4 are also given, for both d^6 and d^7, δ_i, the crystal-field splitting in the ionic near-transition states. One can note that the values of δ and δ_i are not equal, δ_i being larger than δ. So a spin transition occurs for a lower t_{2g}–e_g splitting when covalency is taken into account. This difference between δ and δ_i can be analysed in the framework of a reduction in the Slater integrals of the d orbitals compared with their values calculated for a free ion; the covalent and ionic near-transition states are calculated for the same Slater integrals. Then, the covalent near-transition state corresponds to a splitting δ smaller than the ionic near-transition state. The influence of the Slater integral then appears to be effectively reduced. To obtain, in an ionic calculation, a spin transition at the same splitting δ as in covalent calculations, one has to reduce the Slater integrals by a factor of δ/δ_i.

Table 3. High-spin-to-low-spin transition in the d^6 and d^7 cases. Expectation values of S_z are given for ionic, partly covalent and highly covalent ground states.

	S_z expectation value (units of $\hbar$)		
Configuration	Ionic	Partly covalent	Highly covalent
d^6	1.96	0.95	0.02
d^7	1.42	1.08	0.52

Table 4. High-spin-to-low-spin transition in the d^6 and d^7 cases. Values of total t_{2g}–e_g splitting for covalent and ionic transition states (see the text).

Configuration	Covalent transition sate splitting δ (eV)	Ionic transition state splitting δ_i (eV)
d^6	2.02	2.36
d^7	2.11	2.50

Nevertheless, the analysis of the Hamiltonian eigenstates involved in the covalent and ionic transition shows that they are quite different.

In both the d^6 and the d^7 cases, the ionic near-transition state is a thermal admixture of pure high-spin and pure low-spin states. On the contrary, covalent near-transition states are formed by eigenstates which have intermediate spins. To explain this difference, one should consider that the near-transition states that we defined are not the exact-transition states defined as the states where S_z is exactly 1.0. Indeed, as d-electron spin–orbit coupling is taken into account the ionic exact-transition state has an intermediate spin [1]. It is the same for the covalent exact-transition state. So, when $S_z = 1.0$, both covalent and ionic states have intermediate spins but, as we checked, the path through states of intermediate spins proves to be very abrupt for the ionic transition whereas it is quite smooth for the covalent transition. So, as the near-transition states are not exactly of spin $S_z = 1.0$, the covalent near-transition states are formed by eigenstates which still have intermediate spins opposite to those of the ionic near-transition state which is a thermal admixture of nearly high-spin and nearly low-spin states.

So, even if they have the same S_z expectation value, the covalent and ionic near-transition states are then very different. This strong difference in the initial states produces strong differences in the associated spectra (figures 13 and 14). Once again the differences between the ground states are demonstrated in the spectral shape.

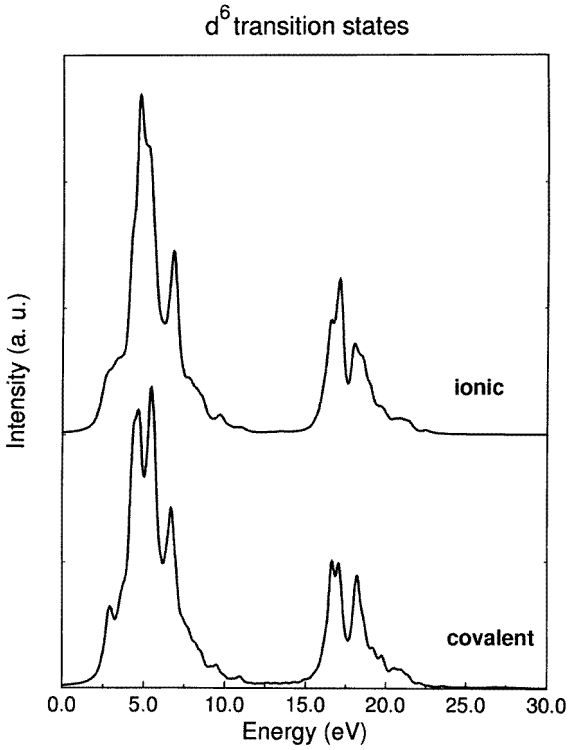

Figure 13. High-spin-to-low-spin transition in the d^6 case (a.u., arbitrary units): lower curve, 2p x-ray absorption spectrum associated with the covalent transition state; upper curve, 2p x-ray absorption spectrum associated with the ionic transition state.

The main information that we can deduce from this comparison of the ionic and covalent transitions is that it is not possible to reproduce, in ionic calculations, the effect of covalency by increasing the crystal field and reducing the Slater integrals.

The fact that reducing Slater integrals cannot always account for the effect of covalency should not forbid the use of such a reduction to reproduce experimental spectra. We have already mentioned ionic calculations of experimental spectra where reducing the Slater integrals was necessary to achieve fitting of calculated spectra to experiment [3, 16–18]. Such a situation occurs also for covalent calculations; for instance in a former study on Ti $L_{2,3}$ edges in different forms of TiO_2 we had to choose a reduction coefficient of 60% [6].

So this reduction coefficient should be regarded as a full parameter of the calculations. Our present calculations show that, once this parameter has been fitted in ionic calculations, the value determined cannot be supposed to apply in calculations including charge transfer. This point parallels the fact that crystal-field splittings obtained by fitting experimental spectra with ionic calculations are different from those obtained with charge-transfer calculations.

The conclusion of our study on this point is that reducing Slater integrals may prove necessary to reproduce experimental spectra, but appears to be insufficient to account for covalency effects.

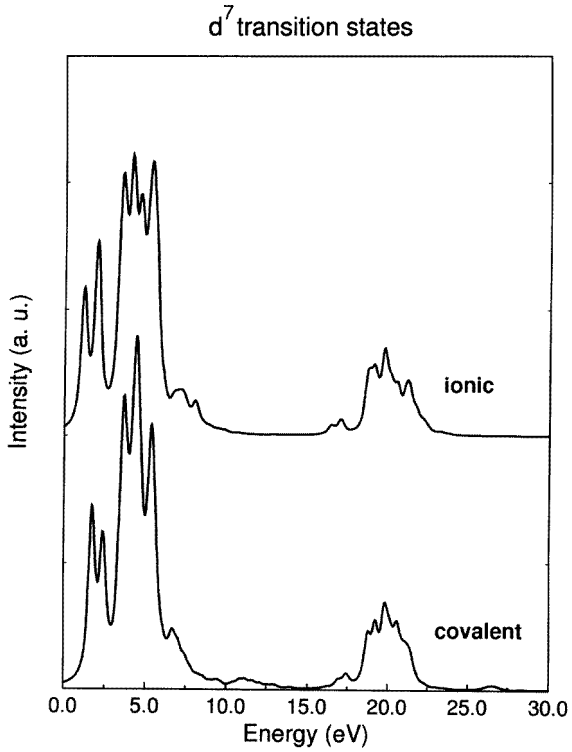

Figure 14. High-spin-to-low-spin transition in the d^7 case (a.u., arbitrary units): lower curve, 2p x-ray absorption spectrum associated with the covalent transition state; upper curve, 2p x-ray absorption spectrum associated with the ionic transition state.

5. The d^8 case

The inclusion of charge transfer produces two effects in the d^8 case. Firstly clear charge-transfer satellites appear and increase in intensity when the covalency is increased. Secondly a narrowing of the structure of the bonding states peaks occurs when the charge transfer is increased.

These effects have been experimentally evidenced on various Ni dihalides and theoretically analysed by van der Laan *et al* [20]. In this paper, the reduction in bonding-state splittings is explained by a reasoning that we believe would be useful to recall briefly.

In a first approach the bandwidth of the ligand hole is neglected. The final states are mixtures of $\underline{c}d^9$ and $\underline{c}d^{10}\underline{L}$ configurations. $\underline{c}d^9$ is composed of numerous states because of spin–orbit and electronic interactions. However, the $\underline{c}d^{10}\underline{L}$ configuration has only two states corresponding to $2p_{1/2}$ and $2p_{3/2}$ holes. So, for each edge, the $\underline{c}d^9$ states mix with only one state. The hybridization will then cause the splitting of the bonding states to decrease compared with the ionic $\underline{c}d^9$ state splitting. The more hybridization there is between the $\underline{c}d^9$ states and the $\underline{c}d^{10}\underline{L}$ state, the more reduced the splitting is. For details about this reduction effect see [20]. This explains nicely the narrowing of the structures of bonding peaks for d^8 spectra.

This narrowing effect can be reproduced by reducing the d–d and p–d Slater integrals measuring the electronic interactions. The fact that reducing the Slater integrals can

reproduce the effect of covalency is a specific feature of the d^8 case. Indeed, we stress the particularity of this case; the reason for the reduction in the splittings is that there is only one state, for each edge, in the configuration $\underline{c}d^{10}\underline{L}$. On the contrary, in the other cases, the $\underline{c}d^n$ and $\underline{c}d^{n+1}\underline{L}$ configurations are both split into many different states by spin–orbit, crystal-field and electronic interactions. The splitting of the $\underline{c}d^{n+1}\underline{L}$ configuration is not, in the general case, small compared with that of the $\underline{c}d^n$ configuration. So the splitting of the bonding states obtained by hybridization can by no means be supposed to be smaller than the ionic splitting. And indeed no such effect can be seen in our spectra.

We stress once again that the reduction in electronic interaction Slater integrals in ionic calculations reproduces nicely the change in spectra which is a specific feature of the d^8 case, as it is made to mimic the reduction in ionic splittings. Of course, even in the d^8 case, the appearance of charge-transfer satellites cannot be obtained by ionic calculations.

6. Conclusion

In this paper we have shown the influence of charge transfer on the $L_{2,3}$ spectral shape for 3d TMOs. It induces a more complex spectral shape and a change in balance between the main peaks. The first effect is due to the appearance of small charge-transfer satellites that cannot be reproduced with ionic calculations. The second is due to a change in the covalent ground state as in the bonding final states. Even if cation $L_{2,3}$ spectra are strongly dependent on atomic effects, we have stressed the importance of covalency effects that should not be neglected.

The study of high-spin-to-low-spin transition in the d^6 and d^7 cases enabled us to highlight the fact that the effect of covalency cannot be reduced to an increase in t_{2g}–e_g splittings and a supplementary reduction in the Slater integrals; so ionic calculations including these two effects cannot reproduce all the aspects of the effect of covalency. Nevertheless this reduction coefficient should be regarded as a parameter of the calculations. The values of this parameter obtained from ionic calculations should be handled carefully when making covalent calculations.

A last point should be mentioned when considering fitting calculations to experimental spectra. Even if ionic calculations happen to fit the experimental spectrum with the same accuracy as a calculation including charge transfer, as the latter takes more physical phenomena into account, it allows a more accurate description of the physical phenomena involved in the electronic structure.

References

[1] For a review see de Groot F M F 1994 *J. Electron Spectrosc. Relat. Phenom.* **67** 529
[2] de Groot F M F, Fuggle J C, Thole B T and Sawatzky G 1990 *Phys. Rev.* B **42** 5459
[3] van der Laan G and Kirkman I W 1992 *J. Phys.: Condens. Matter* **4** 4189
[4] Okada K and Kotani A 1993 *J. Electron Spectrosc. Relat. Phenom.* **62** 131
[5] van Veenendaal M and Sawatzky G 1994 *Phys. Rev.* B **50** 11 326
[6] Crocombette J P and Jollet F 1994 *J. Phys.: Condens. Matter* **6** 10 811
[7] Crocombette J P and Jollet F 1994 *J. Phys.: Condens. Matter* **6** 8341
[8] Crocombette J P, Pollak M, Jollet F, Thromat N and Gautier-Soyer M 1995 *Phys. Rev.* B **52** 3143
[9] Teo B K and Lee P A 1979 *J. Am. Chem. Soc.* **101** 2815
[10] Slater J C and Koster G F 1954 *Phys. Rev.* **94** 1498
[11] de Groot F M F, Fuggle J C, Thole B T and Sawatzky G 1990 *Phys. Rev.* B **41** 928
[12] Cowan R D 1981 *The Theory of Atomic Structure and Spectra* (Berkeley CA: University of California Press) p 464
[13] Tanaka A and Jo T 1992 *J. Phys. Soc. Japan* **61** 2040

[14] Griffith J S 1961 *The Theory of Transition Metal Ions* (London: Cambridge University Press) p 234
[15] Thole B T and van der Laan G 1988 *Phys. Rev.* B **38** 3158
[16] van Veenendaal M A and Sawatzky G A 1994 *Phys. Rev.* B **49** 3473
[17] Okada K and Kotani A 1992 *J. Phys. Soc. Japan* **61** 449
[18] de Groot F M F, Hu Z W, Lopez M F, Kaindl G, Guillot F and Tronc M 1994 *J. Chem. Phys.* **101** 6570
[19] Jørgensen C K 1962 *Orbitals in Atoms and Molecules* (London: Academic)
[20] van der Laan G, Zaanen J, Sawatzky G A, Karnatak R and Esteva J M 1986 *Phys. Rev.* B **33** 4253